ELSEVIER

Contents lists available at ScienceDirect

## **Materials Today Communications**

journal homepage: www.elsevier.com/locate/mtcomm





# Thermoset polymer composites with gradient natural and synthetic fiber reinforcement: Self-healing, shape-memory, and fiber recyclability

Sakil Mahmud<sup>a</sup>, John Konlan<sup>a</sup>, Jenny Deicaza<sup>a</sup>, Rachel Anna Schmidt<sup>a,c</sup>, Guoqiang Li<sup>a,b,\*</sup>

- a Department of Mechanical and Industrial Engineering, Louisiana State University, Baton Rouge, LA 70803, United States of America
- b Department of Mechanical Engineering, Southern University and A&M College, Baton Rouge, LA 70813, United States of America
- <sup>c</sup> Department of Chemistry, College of Natural Sciences, The University of Texas at Austin, Austin, TX 78712, United States of America

## ARTICLE INFO

Keywords: Renewable fibers Synthetic fibers Self-healing Composite laminates Recyclability

## ABSTRACT

Natural fibers have high potential as renewable reinforcement for polymers; however, their lower load-carrying capacity compared to synthetic fibers significantly limits the wide application in fiber-reinforced polymer composites. In laminated composite beams under bending load, the normal stress is the highest on the top and bottom layers but is zero at the mid-plane, with almost a linear normal strain distribution. Although the shear stress is the highest at the mid-plane, it may not be a major concern as most polymers can survive the high shear stress. Using this concept, we have designed a hybrid fiber reinforcement in a gradient manner: from the surface to the mid-plane were carbon fiber, glass fiber, and natural jute fiber, respectively. A newly synthesized self-healable shape memory polymer was used for laminating the fibers. Performance characterizations demonstrated that even using a significant amount of natural fibers in the composites, the samples with gradient fiber reinforcement showed competitive mechanical properties to fully carbon or glass fiber reinforced composites and much higher mechanical properties than the composite prepared with entirely natural fibers or glass fibers. For example, the gradient composites show up to 550 % flexural strength of the composites made of fully natural fibers, and around 14 % and 34 % higher flexural strength than that of the composites made of pure glass and pure carbon fibers, respectively. In addition, the composites retain excellent self-healing, shape-recovery, and fiber-recycling properties.

## 1. Introduction

Polymers or plastics are necessary for many facets of contemporary life, including but are not limited to uses in buildings, vehicles, wind turbine blades, healthcare, lightweight structures, and textiles. Polymers have several advantageous qualities as compared to other materials. For instance, depending on the polymer type, it is possible to heat, sterilize, and handle plastics while keeping their structural integrity [1]. The apparent effects of our addiction to single-use plastics are everywhere, from bags stuck in hedgerows to bottles bobbling in the sea. We are all aware of the severe consequences of plastic pollution. However, the precise way in which plastics contribute to climate change and global warming is less well discussed [2]. People often believe that climate change and plastic pollution are two distinct problems, and they are occasionally even seen as rival issues. However, in critical evaluation, they are fundamentally linked to each other. For example, if we search for the link between climate change and plastic pollution in the ocean, it

could be found in three overarching ways [3]. (a) Plastic manufacturing uses fossil fuels and scarce resources. The end-of-life (EOL) of plastic waste contributes expressively to global greenhouse gas emissions (GHG), and although bio-based plastics are likely to expand in manufacturing, their sustainability and GHG contribution are also questionable [4]. (b) The environment accelerates the distribution of plastic pollutants, which will continue as extreme weather events and flooding and drought become more frequent due to the changing climate [5]. (c) The effects of plastic waste on species and ecosystems are also becoming more and more evident as being detrimental to them. In contrast, the impact of global warming alone has demonstrably disastrous effects on the marine environment [3].

According to our understanding, some options can be proposed to overcome/minimize plastic pollution, but face challenges. (a) Recycling and reusing existing plastics is challenging since waste plastic commonly contains different polymer types and non-plastic substances like additives [6]. (b) The production of eco-friendly polymers from renewable

<sup>\*</sup> Corresponding author at: Department of Mechanical and Industrial Engineering, Louisiana State University, Baton Rouge, LA 70803, United States of America. E-mail address: lguoqi1@lsu.edu (G. Li).

resources is a promising bio-based substitute for petroleum-based plastic [7]. However, the challenges underlying their production, application, and consumer satisfaction regarding mechanical properties prevent them from wide acceptance [8]. (c) The composition of existing fossil-based/traditional plastics with biobased polymers [9] or renewable resources such as plant fibers [10] has been conducted. For example, using 30 wt. % renewable natural fibers in plastic products is ultimately a 30 wt. % reduction of plastic consumption and pollution. However, when discussing fiber-reinforced polymer (FRP) composites, the inorganic fibers such as carbon, glass, etc., or other polymeric fibers, such as nylon, come in the front line due to their high strength and availability. Especially due to their high mechanical properties, many materials have been hybridized with synthetic fiber reinforcements. For example, Muflikhun et al. added general steel in carbon fiber reinforced polymer to increase the load carrying capacity of the laminates by delaying the failure in terms of strain [11]. The same group has also analyzed the mechanical properties and explored the failure mechanism of different inorganic fiber-reinforced polymers [12]. Nevertheless, the objectives for the reduction of plastic consumption and plastic pollution remain evaded. On the other hand, although natural fibers are renewable, cheap, and biodegradable, they cannot compete with synthetic fibers in terms of machinal properties [13]. Our previous report observed that only 10 wt. % use of cellulose fibers in the polylactide composites causes up to  $\sim$ 27 % reduction in tensile strength [14].

Driven by cost and mechanical properties, hybrid fiber reinforcement has been used in laminated composites. In the synthetic-synthetic hybrid fibers reinforced composites, (i) Dong et al. [15] examined the flexural strength of glass/carbon FRP composites. Due to a localized compressive load in the three-point bending test, the compression side was crushed, and the bottom surface showed tensile failure. It was unknown how hybridization affects structural strength. (ii) Ferrante et al. [16] examined basalt/carbon FRP composites where the flexural characteristics were tested quasi-statically. Acoustic sensors detected localized fractures when samples were loaded. This method detects instant delamination (internal cracks) during testing but cannot specify the damage location. (iii) Yan et al. [17] examined the low-velocity impact of Kevlar/glass FRPs composites. The samples were subjected to impacts from both bursting probes and drop-weight impactors. The result demonstrates that the fiber density indeed influenced the samples' impact resistance. On the other hand, in the natural-synthetic hybrid fibers reinforced composites, (i) Sarasini et al. [18] examined the failure process of low-velocity impact damage of carbon/flax (natural fiber) FRPs composites, where the wt. % of carbon fibers merely dominated the flexural modulus. (ii) Gangil et al. [19] examined the carbon/flax fibers reinforced polymers and observed that the damping properties were improved, but tensile strength dropped. The damping coefficient was four folds higher than that of a composite prepared with carbon fiber alone. The findings were identical to the other synthetic, and natural hybrid fibers reinforced polymer composites [19]. (iii) In addition, Nugraha et al. reviewed a number of articles on the binary composites made with natural fibers mixed with carbon fiber or glass fiber in terms of mechanical properties such as flexural strength, tensile strength, hardness, and fatigue [20].

Theoretically, in laminated composite beams under bending load, the normal stress is the highest on the top and bottom layers but zero at the mid-plane, with almost a linear slope. Although the shear stress is the highest at the mid-plane, it may not be a primary concern as most polymers can survive the high shear stress. Based on this concept, we have designed a hybrid fiber reinforcement in a gradient manner: from the surface to the mid-plane were the strongest carbon fiber, strong glass fiber, and lower strength natural jute fiber, respectively. Herein, a newly synthesized room-temperature self-healable, recyclable, and shape-recoverable thermoset polymer was used for laminating the fibers in a gradient arrangement. This polymer has been chosen because its thermoset network is covalently and mildly cross-linked from a low molecular weight branched polyethylenimine (PEI) and an ester-containing

epoxy monomer (diglycidyl 1,2-cyclohexanedicarboxylate (DCN)). The entire synthesis route of the polymer is redrawn in Fig. 1, based on our previous report [21]. The abundant primary amine terminals and secondary amines on branched chains of the DCN-PEI network produced hydroxyls and innate ester groups that can produce significant but loosely packed multiple hydrogen bonds, which results in supportive noncovalent cross-linking of the network. Therefore, the resulting polymer is mechanically strong and chemically and thermally stable because of the twin cross-linking processes. The glassy thermoset polymer resulting from the ruptured hydrogen bonds can offer self-healing function at room temperature due to the excess mobility of the chain branches and ends. Although some of the broken covalent bonds cannot be re-established at room temperature, the recovery of the dense hydrogen bonds can be sufficient to achieve a reasonable healing efficiency. However, thermoset polymers often pose an additional challenge for recyclability due to their everlasting cross-link structure and inability to be melted down [22]. Our previous study shows that this polymer can be easily dissolved in alcohols through catalyst-free transesterification owing to the intrinsic catalytic action of the tertiary amines within the network [21]. This study aims to prepare a hybrid carbon/glass/jute fiber reinforced DCN-PEI laminated composite by arranging the fibers in a gradient manner and testing their mechanical, thermal, and recycling properties.

## 2. Experimental

#### 2.1. Materials

Low molecular-weight branched polyethyleneimine (PEI, average  $M_w \sim 800$  by LS, average  $M_n \sim 600$ ) and ester-containing epoxy monomer diglycidyl 1,2-cyclohexanedicarboxylate (DCN) were purchased from Sigma-Aldrich and used as received. A mold release agent (fib-release) and the synthetic reinforcement fabrics (made of unidirectional glass fibers and unidirectional carbon fibers) were purchased from Fiberglast, USA. A burlap fabric made of natural jute fibers was purchased from AAYUTM Burlap Liner Roll, India.

## 2.2. Fabrication of composite laminates

Based on our previous report [21], the thermoset polymers were initially synthesized by a one-pot polycondensation reaction of branched PEI monomers and commercial DCN. In brief, the branched PEI and DCN were mixed homogenously, maintaining a mass ratio of 1:1 in a 500-mL beaker at room temperature. The homogeneous mixture was degassed in a vacuum oven for 15 min to eliminate the bubbles. As shown in Fig. 2, a combination of natural jute (N), carbon (C), and glass (G) fabric were used in a gradient manner (Gradient = CGNNNGC) to prepare the composite laminates. The homogeneous mixture of DCN and PEI was then used to wet the fabrics by hand layup. After laminating the rectangular mold of 5.04 mm thickness with wet fabrics, a pair of Teflon sheets and subsequently a pair of thin aluminum plates over both sides of the mold were clamped by 8 C-clamps. Then the arrangement was cured at room temperature overnight and thermally cured at 100 °C for 2 h and 150 °C for another 2 h. After demolding the assembly, the laminated plate was cut into 6-inch × 1-inch using a water-jet cutting machine (WARDJet  $5' \times 10'$  Waterjet Machining System). Similarly, three other composite laminates of fully 6-layers of unidirectional glass fabric (G6 = GGGGG), 8-layers of unidirectional carbon fabric (C8 = CCCCCCC), and 6-layers of natural jute fabric (N6 = NNNNNN) were prepared as references. It is worth mentioning that the vacuum-assisted resin infusion (VARI) or autoclave processes for preparing composite laminates would offer more commercial scalability and higher quality product. In this study, the hand layup technique was chosen due to its flexibility regarding the size and shape of the composite laminates and the types of fibers, resins, or additives used. In addition, combining hand layup with the hot press technique can increase the fiber volume fraction

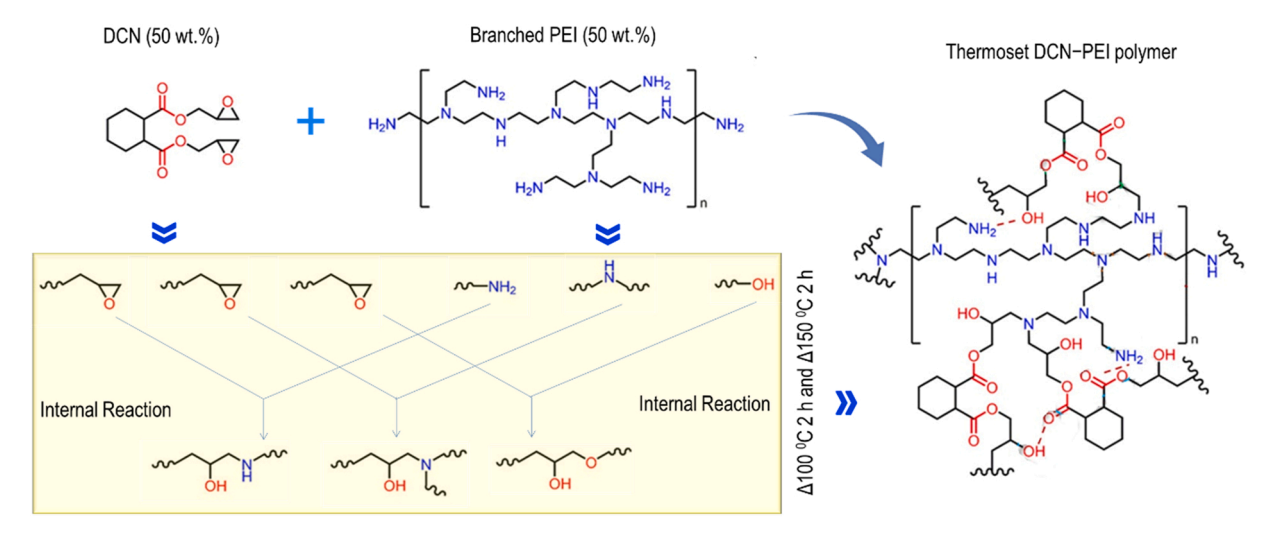


Fig. 1. Synthesis route of DCN—PEI thermoset polymer in a mass ratio of 1:1 (with minor modification, the synthesis process has been redrawn from our previous report [21]).

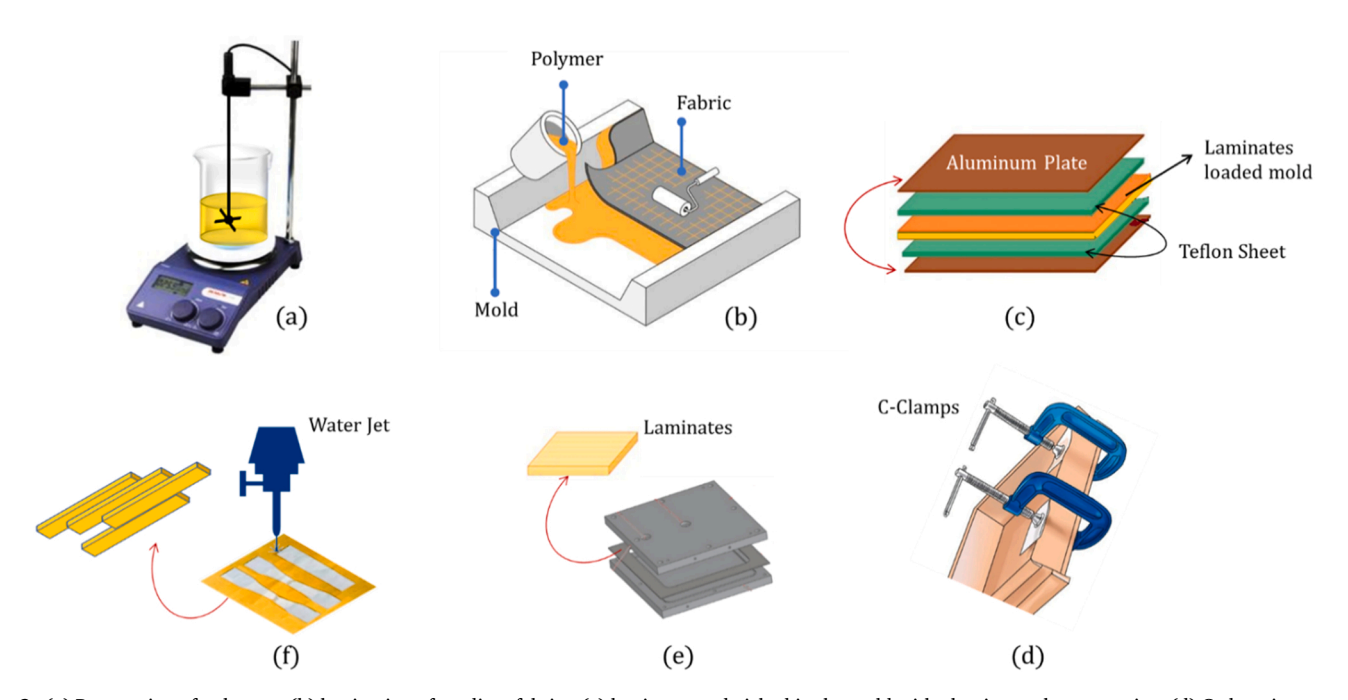


Fig. 2. (a) Preparation of polymers, (b) lamination of gradient fabrics, (c) laminate sandwiched in the mold with aluminum plates covering, (d) C-clamping to exert pressure on laminate, (e) demolding the sandwiched laminate after thermal curing, and (f) water jet cutting of laminates into rectangular and dogbone samples.

and the quality of the laminates [23,24].

Recycling fabric from the composite laminates was carried out by immersing the as-prepared gradient composite plate in 200 mL of ethylene glycol (EG) for 3 h at 150  $^{\circ}\text{C}$ . After entirely dissolving the polymer matrix, the collected reinforced fabrics were softly washed with ethanol five times and dried at room temperature overnight. The recycled fabrics were reused by following the same procedure to prepare the regenerated composite laminates.

## 2.3. Characterization and measurements

A Nicolet 6700 FTIR spectrometer from Thermo Fisher Scientific (USA) was used to capture the FTIR spectra, capturing 32 scans from 500 to 4000  $\rm cm^{-1}$ . A PerkinElmer 4000 differential scanning calorimeter (DSC, MA, USA) was used to examine the thermal properties and glass transition temperature (Tg). Nitrogen gas was purged at a rate of 30 mL per minute. About 5–10 mg of the materials were heated at a heating

rate of 20 °C/min from - 50–200 °C in a heat-cool-heat manner. The samples were heated and cooled between - 50 and 200 °C to calculate  $T_g$  at the same rate; the holding times at - 50 and 200 °C were 2 min. To calculate  $T_g$ , the second heating curve was used. To evaluate the thermal stability of the composites, the TGA profiles were obtained using a Q5000 thermal analyzer (TA Co., USA) from 20° to 800°C at a heating rate of 10 °C/min in nitrogen atmospheres with a flow rate of 40 mL per minute. The interfacial compatibility and the delamination between the fabric layers were observed using a polarizing optical microscope (POM, Leitz Laborlux 12 Pol) and captured by an built-in digital camera.

The laminates were evaluated by a three-point bending test on the Q-TEST 150 MTS machine at a 2.0 mm/min loading rate. Initially, the test was carried out until sample failure to record the load at maxima. Then the formula  $(\sigma_f\!=\!3PL/2bh^2)$  was used to determine the flexural stress  $(\sigma)$  at any point on the load-deflection curve that occurs at the outer surface at mid-span. Herein, P was the maximum applied force, L was the span length, b was the sample width, and h was the sample thickness.

Similarly, the maximum strain ( $\epsilon=6\delta h/L^2$ ) at the outer surface occurs at mid-span was calculated. Herein,  $\delta$  was the mid-span deflection. To determine the damage healing capability, the bending tested samples were pressed with the same pressure under a free boundary condition at 140 °C for 2 h followed by room temperature cooling. By running four cycles of 3-point bending tests on healed samples, it was possible to determine the repeatability of healing and the healing efficiency [ $\eta=(\sigma_H/\sigma_V)\times 100$  %]. Herein,  $\sigma_V$  was the maximum flexural stress of the virgin samples, and  $\sigma_H$  was the maximum flexural stress of the healed samples.

To evaluate the shape memory behavior, a rectangular composite  $(152.40 \times 25.40 \times 5.08 \text{ mm}^3)$  beam was placed in between the clamps of 3-point bending. Then the sample was bent to 16 mm of deflection at the mid-span at a speed of 2.0 mm/min at room temperature. Then, the bent sample was held for 10 min, followed by load removal, which is the cold programming of the composite laminates, i.e., programming in the glassy state [25,26]. The length of the programmed specimen was measured to calculate the shape fixity ratio. The programmed sample was further maintained at room temperature for 5 min. The entire process is shown in Fig. 1d. To measure the shape recovery ratio, the bent sample was heated at 90 °C for 10 min, and the length of the recovered sample was measured. The following equations were used to calculate the shape fixity ratio  $[F = (\ell_0 - \ell_2)/(\ell_0 - \ell_1) \times 100 \%]$  and the shape recovery ratio [R=  $(\ell_3 - \ell_2)/(\ell_0 - \ell_2) \times 100$  %]). Herein,  $\ell_0$  was the initial length,  $\ell_1$  was the length after bending,  $\ell_2$  was the length after the load removal, and  $\ell_3$  was the length after shape recovery.

#### 3. Results and discussions

## 3.1. Structural characterizations

Initially, the composite density  $(\rho_c)$  was calculated based on constituent (fibers and polymer) densities and their corresponding weight fractions, as  $\rho_c = \left[\sum (Wi/\rho_i)\right]^{-1}$ , whereas,  $W_i$  and  $\rho_i$  were weight fraction and density of the constituting materials, respectively. In addition, the volume fractions (V\_i) of fiber and polymer were calculated as  $V_i = W_i \times \rho_c/\rho_i$ . The results are summarized in Table 1. The fiber volume fraction of all samples was nearly 24.5 %.

The glass transition temperature (Tg) was determined from the slope of the second heating curve (Fig. 3a). Although different fibers were used in different composites, the  $T_{\rm g}$  of the composite was very close to each other since the  $T_g$  value of the composites is dependent on the polymer, not the fibers. Whatever the difference in Tg values, they carried significant information that should be discussed. Herein, the Tg of the pure DCN-PEI polymer was found to be about 38.07 oC, whereas the composites have shown slightly lower Tg. In the presence of natural jute fiber, glass fiber, carbon fiber, and their combination showed the Tg of N6, G6, C8 and gradient composites around 32.19, 33.06, 35.73, and 35.09 oC, respectively, which are lower than the pure DCN-PEI polymer (38.07°C). It means the N6 and G6 composites record the largest decrease in Tg among all samples. Generally, lamination or coating of the fiber due to the interfacial attraction in FRPs limits the segmental movement in the interface, restricts the mobility of the polymer chain, and grows the cross-linking density between fibers and the polymer chain [27]. As a result, the Tg of the polymer mtrix should be increased due to the reinforcement by fibers, but the opposites phenomenon was

observed here. Such a decrease in  $T_g$  to the lower temperature might be attributed to the increased local mobility of the polymer molecules between the fibers and the matrix [28]. Hence, the glass transition starts at lower temperatures. The addition of a single type of fibers in the FRPs caused a decrease in the  $T_g$ . Nevertheless, in the gradient composites, when comparing single-type fiber reinforcement, the  $T_g$  was increased with respect to N6 and G6 composites and comparable with C8 composites.

TGA was carried out to investigate the thermal stability of the pure polymer and composites. The samples' remaining weight percentages as a function of temperature are shown in Fig. 3b. Significant parameters such as the temperature of 5 % weight loss ( $T_{5\%}$ ) (usually considered as the temperature at which deterioration begins), the temperature of maximum degradation rate (Tmax), and the char yield after the experiment are summarized in Table 2. It was observed that all composites, including pure polymer (except natural fiber contained laminates), lost up to ~6 % weight at 150 °C. It was reasonable to demonstrate good thermo-oxidative stability at maximum curing temperature (150 °C). However, the sample contained natural fiber, i.e., N6 and gradient composites, showing higher weight loss (~11 %) at maximum curing temperature. This is because jute fibers are highly hydrophilic in nature and can retain up to 5 % moisture. A similar weight loss pattern was also observed while calculating  $T_5$  % and  $T_{max}$ . Almost all samples follow three-step weight losses. In the first step, around 5 % of weight loss at 150 °C can ascribe to the loss of bonded trace water molecules. The second weight loss occurs from 260 °C to 400 °C, resulting in a 70 % weight loss ascribed to the depolymerization, dehydration, and degradation of polymers. In the final step, weight loss occurs above 410 °C resulting in another major weight drop up to char formation. This is due to the oxidation of the remaining char residue and subsequent breakdown into small volatile molecules. A similar pattern of degradation was also reported for other polymers and composites [29]. Moreover, the char yield by gradient sample at 400 <sup>0</sup>C was significantly higher than pure polymer, N6 and C8 composites. The increase in char yield correlates positively with flame retardancy. Thus, increased char formation can inhibit the production of combustible gases, lower the exothermicity of the pyrolysis reaction, and prevent the thermal conductivity of burning materials [30,31].

Furthermore, the Coats-Redfern approach [32] has been used to analyze the TGA data in order to determine the activation energy needed for the thermal decomposition process. The Coats-Redfern technique states that the mathematical relation for a first-order reaction is:

$$\log\left[\frac{-\log(1-\alpha)}{T^2}\right] = \log\frac{AR}{\beta E_a}\left[1 - \frac{2RT}{E_a}\right] - \frac{E_a}{2.303RT}$$

Herein, T is the absolute temperature,  $\beta$  is the linear heating rate, A is the frequency factor,  $E_a$  is the activation energy, R is the gas constant, and  $\alpha$  is the fraction of decomposed sample at time t represented by  $\alpha=(W_0-W_t)/(W_0-W_f),$  where  $W_0$  is the initial sample weight (prior to the decomposition reaction),  $W_t$  is the sample weight at any given temperature and  $W_f$  is final sample weight after completion of the reaction. Finally, the activation energy was calculated by linear fitting to log  $[-\log(1-\alpha)/T^2]$  vs 1000/T plot (Fig. S2 and Table S1 in Supplementary Information). The calculated activation energy was around 20 KJ/mol (Table 2), which is much lower than other natural fiberreinforced polymers [33]. It is worth mentioning that the activation

**Table 1** Formulation of composites.

Sample Name	Fabric density (g/cm <sup>3</sup> )	Fiber wt. fraction (%)	Matrix wt. fraction (%)	Fiber vol. fraction (%)	Matrix vol. fraction (%)	Composite density (g/cm <sup>3</sup> )
N6	1.49	27.39	72.61	24.04	75.96	1.31
G6	2.25	38.51	61.49	25.81	74.19	1.51
C8	1.75	30.31	69.69	23.70	76.30	1.37
Gradient	1.89	33.49	66.51	24.95	75.05	1.41

The pure DCN-PEI polymer density was 1.25 g/cm<sup>3</sup>.

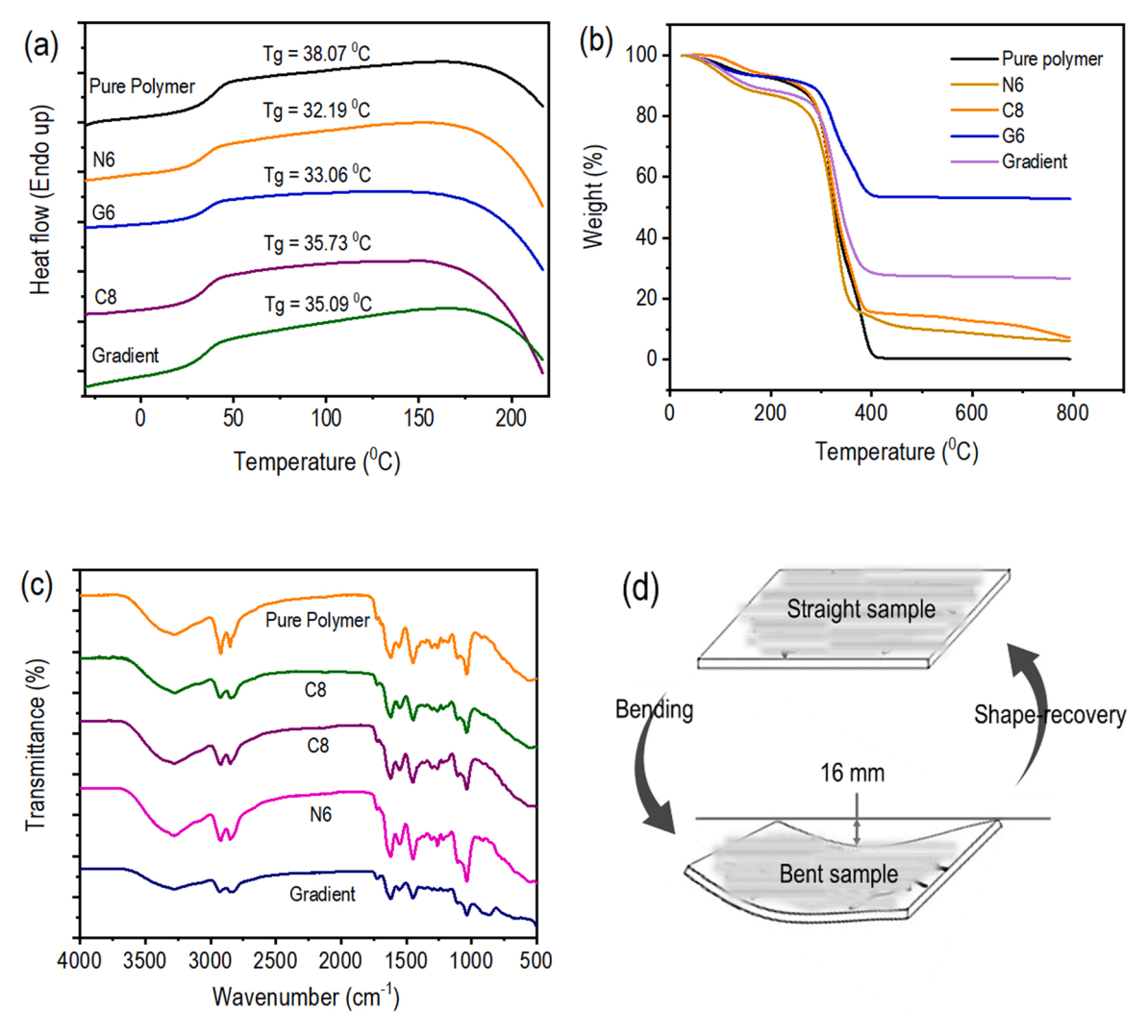


Fig. 3. (a) DSC second heating scan, (b) TGA curves, (c) FTIR spectra, and (d) shape-recovery scheme of composites.

**Table 2**Thermal properties of composites based on DSC and TGA.

Samples	T <sub>g</sub> (°C)	wt. % loss @ 150 °C	T <sub>5 %</sub> ( <sup>0</sup> C)	T <sub>max</sub> (°C)	Residue wt. % @ 800 °C	E <sub>a</sub> (kJ/mol)
Pure polymer	38.07	6.09	128.19	345.47	0.16	20.78
N6	32.19	10.98	91.12	320.12	6.10	20.72
G6	33.06	6.33	117.57	361.81	52.75	20.73
C8	35.73	4.91	143.13	318.53	7.14	19.99
Gradient	35.09	10.98	104.83	336.68	26.67	20.74

energy is a barrier that must be overcome before a chemical reaction can occur, and greater activation energy indicates more difficulty for a reaction to occur. It establishes the sensitivity and responsiveness of a reaction rate [34].

The interaction between fiber and polymer was evaluated using FTIR spectra (Fig. 3c). In the pure DCN-PEI polymer, the absence of an epoxy group (centered around 902 cm<sup>-1</sup>) represents the complete curing of the epoxy group by thermal cross-linking [21]. The pure polymer showed the abundant H-bonds attributed to –NH, –OH, and C=O moieties in the DCN-PEI polymer network. However, all laminates composite revealed similar spectra to pure polymers. The absence of peak change suggests the lack of chemical interactions between the fibers and the polymer matrix, and only the physical embedment of the fibers in the polymer matrix. This phenomenon was also observed in previous reports [35,36].

Numerous variables, such as the fiber orientation, ply stacking sequency, types of fibers, individual fiber strength, compression pressure during hand layup process, etc., can alter the mechanical properties of FRP composite [37]. In this study, three-point bending testing was used to examine mechanical features in relation to types of fibers and their gradient arrangement. A typical load-deflection plot is shown in Figs. S3 and S4. The average (of four tests) peak bending loads for the N6, G6, C8 and gradient composites were respectively  $32.41 \pm 1.24$ ,  $175.65 \pm 17.04$ ,  $326.83 \pm 37.72$ , and  $238.16 \pm 57.28$  N. Among the three composites of with single type of fibers, it was expected that C8 composites should have the highest bending loads followed by G6 composites, and the lowest should be the N6 composites. This is exactly the case, as given in Table S2 and Fig. 4. It is also expected that the gradient composites, due to its large portion of natural fibers, should have lower flexure strength than C8, and even lower than G6 composites.

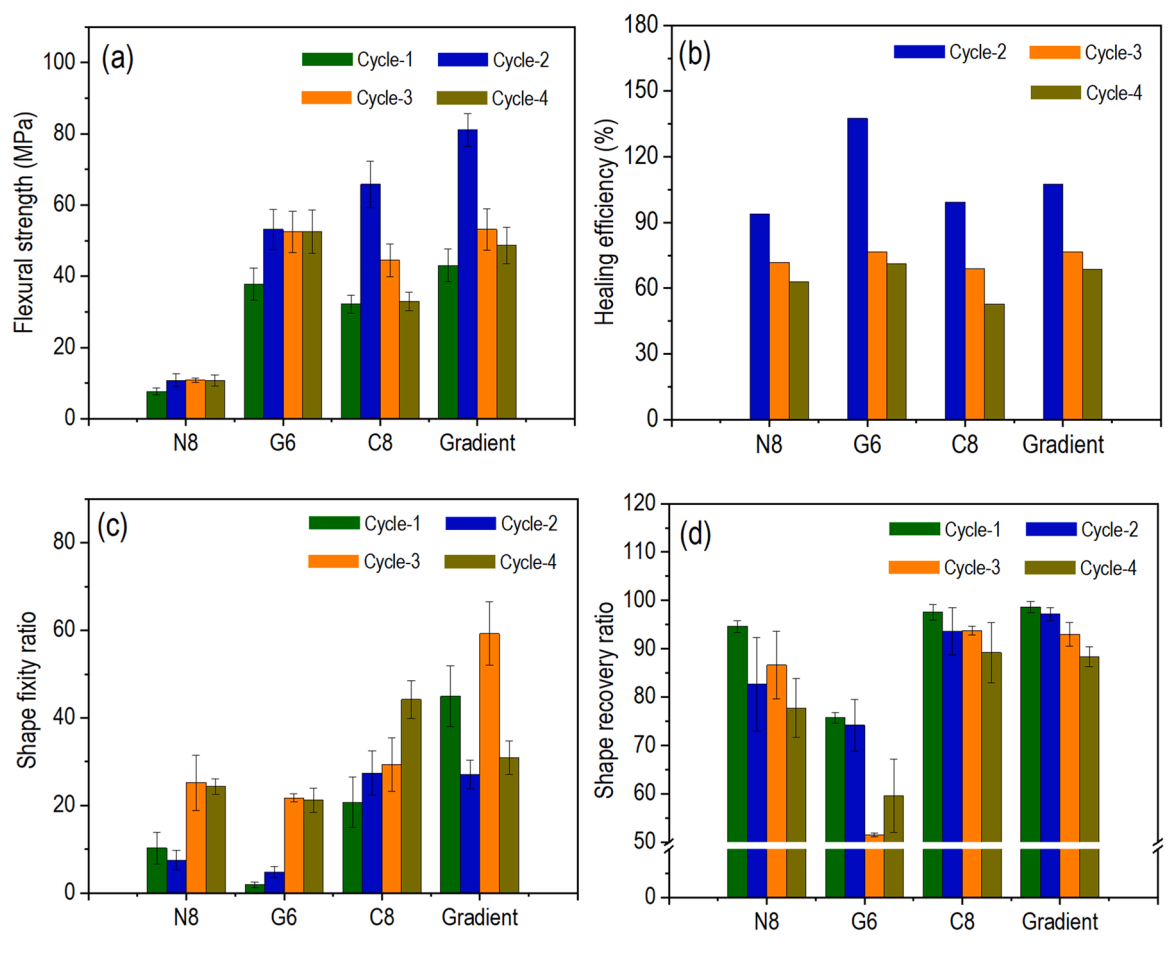


Fig. 4. Flexural strength  $(\sigma_f)$ , healing efficiency  $(\eta)$ , shape fixity ratio (F), and shape recovery ratio (R) of composites based on three-point bending tests.

However, this is not the case. The gradient composites have flexure strength slightly higher than that of C8 and G6 composite. This is because the gradient arrangement of fibers in the composites matches the flexure stress distribution (the normal stress is the highest on the top and bottom layers but is zero at the mid-plane, with almost a linear slope) in the laminated composite beam: the top and bottom-most layers with strongest carbon fibers, then comparatively less strong glass fibers in the inner layers, and the weakest natural fibers in the mid-layers. Although the shear stress is the highest at the mid-plane under three-point beaning configuration, it may not be a major concern as most polymers can survive the high shear stress [38]. Moreover, if the laminated beam is under four-point bending test, the beam will be subjected to pure bending stress in the mid-span, with zero shear stress. Therefore, our idea of using hybrid fiber reinforcement and arranging them in gradient order from the surface to the mid-plane, has retained and exceeded the mechanical properties of C8 and G6 composites. In other words, the renewable but weak natural fibers can be used in load carrying structures.

## 3.2. Self-healing and shape recovery effect

In laminated fiber-reinforced polymer composites, delamination is a significant cause of failure. The combination of extremely low through-thickness strength and significant interlaminar stresses results in the creation of delamination. Therefore, the three-point bending test on FRP laminates was conducted to demonstrate the self-healing of delamination at room temperature and the temperature above the  $T_g$ . The composite samples were initially delaminated by three-point bending, then healed by compression of 4 MPa pressure for 2 h at 140  $^{\circ}\text{C}$ . To assess the effectiveness of self-healing, the damage/healing cycle was conducted

four times, and the associated data were recorded in Table S2 and plotted in Fig. 4. All composites but N6 samples exhibited evident delamination and bending-induced matrix cracks (Fig. S5). The fracture of the polymer matrix was evident by the wide-opened delamination. Nevertheless, the reason for exhibiting no visible delamination in N6 composites could be associated with the high flexibility of natural fibers. The softness and flexibility of natural fibers can assist in reducing the stress concentration at the fiber/matrix interface. When a composite material is subjected to mechanical loading, stresses tend to concentrate at the interface between the fibers and the matrix, which can lead to debonding and delamination. Soft and flexible fibers can deform and distribute the stress more evenly, reducing the stress concentration at the interface and mitigating the likelihood of delamination. In addition, the delaminated samples were observed by an optical microscope to visualize the delamination. Significant delamination between the fiber layers was found (Fig. 5). However, after compressing the delaminated specimen, almost no gap between the fiber layers can be observed visually and microscopically, indicating a good healing response. This self-healing property is ascribed to the excellent mobility of the produced numerous hydrogen bonds connected to the PEI backbone, which can reconnect fractured networks through the rearrangement of dynamic hydrogen bonds. To understand the self-healing performance numerically, flexural strength  $(\sigma_f)$  and healing efficiency  $(\eta)$  were calculated and presented in Table S2, as well as plotted in Fig. 4. It was worth noting that the flexural strength of all samples increased in the second cycle and was followed by a systematic drop in the subsequent cycles. In the second cycle, a similar pattern was observed in healing efficiency, exceeding 100 % of n for G6 and gradient composites. The samples were pressed by C-clamps during the fabrication of the composites and thermal curing. It is believed that the pressure was

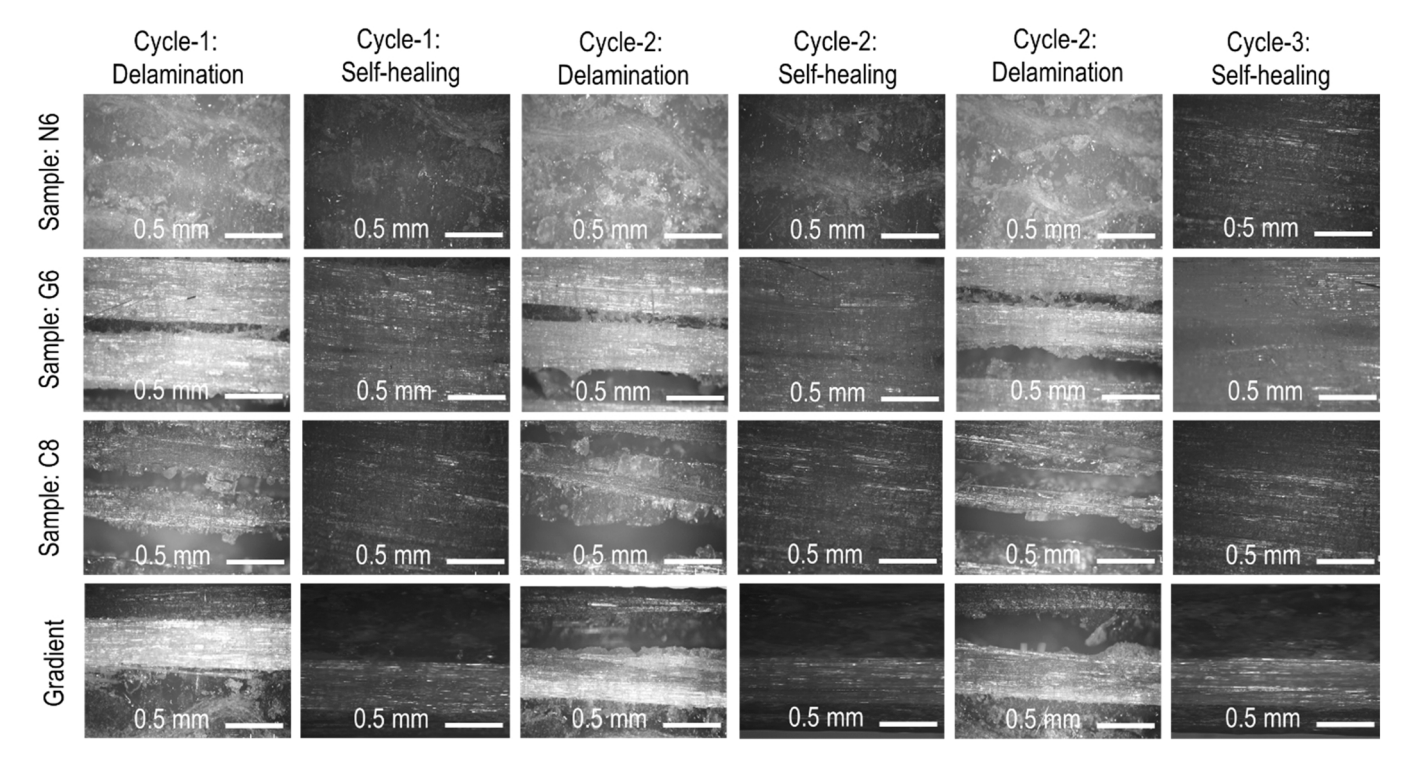


Fig. 5. Microscopic view of delamination and healed area of the composites samples.

insufficient to condense the composites during manufacturing. In the second cycle, the 4 MPa pressure at a high temperature not only helped delamination healing but also made the laminates denser, increasing flexure strength. In the subsequent cycles, the effect of densification no longer exists, leading to normal tendency, i.e., the flexure strength and the healing efficiency decreased as the damage/healing cycle increased.

The bending deformation at the rubbery state was used as a fundamental measurement to assess the shape memory properties. A cycle of bending programming and recovery is shown in Fig. S1. The shape fixity ratio (F) and shape recovery ratio (R) were calculated based on bending deformation and summarized in Table S2, as well as plotted in Fig. 4. All samples but G6 composites showed ~95 % shape recovery ratio in the first cycle. The shape recovery ratio of G6 is the lowest in the first cycle, which is about 75 %. As shown in Fig. S5, the glass fiber fractured after the first bending at the bottom layer, which significantly lowered the shape recovery ratio. For the other composites, for example, C8, although there are two large delamination after the first bending, the carbon fibers in the bottom ply are still intact. Therefore, C8 composites still have large shape recovery ratio. For the gradient composite, it is seen that the top layer has a local buckling after the first bending. Because no fiber fracture occurred, the shape recovery ratio is the highest. As the number of bending cycles increased, the shape recovery ratio for all composites decreased, which may be due to the irreversible structural failure of individual fibers. In the case of shape fixity ratio, although all the composites have lower shape fixity ratios, the gradient composite is the highest after the first bending programming. The local buckling at the top layer resists the spring-back of the bent laminate, leading to a larger shape fixity ratio. The overall shape memory performance indicates that the gradient composites have the best shape memory properties among all the composites.

## 3.3. Recyclability of composite laminates

DCN-PEI is a promising matrix for fabricating high-performance recyclable fiber-reinforced composite laminates due to its robust mechanical properties and dynamic cross-linked network. Recycling fibers is crucial in practical applications due to their extensive usage, large

energy consumption, and high cost in reinforcing high-performance load-carrying engineering structures. Unfortunately, recycling fiber from the fiber-reinforced thermoset polymer composite laminates is a challenging process due to the cross-linked nature of the polymer matrix. Thermosetting polymer matrices cannot be gently melted or dissolved as thermoplastic polymer does because of their inherent characteristics, i.e., their irreversible three-dimensional cross-linked network structure. However, due to the covalent adaptable network (CAN) of the polymer [21], the thermoset polymer matrix can be recycled, including wet-recycling by solvent [39]. Herein a commonly used approach has been adopted, i.e., separating the fibers from the polymer matrix using a solvent, cleaning, and sorting the fibers, and reprocessing the fibers for re-composition [40,41]. Fig. 6a depicts the chemical recycling process of gradient composite laminate by immersion of the laminate in EG at 150 °C for 3 h. After gradually dissolving the polymer matrix in EG, followed by washing and drying, the clean fiber can be separated. Using an optical microscope, the morphologies of both the virgin and recycled fabrics were observed (Fig. 6b). The recycled fabric has the same pattern as the original fabric and has no visible loose fibers. It can also observe that there is a negligible amount of polymer residue adhered to the fiber surface but no damage or change in fiber dimension. The presence of  $\beta$ -hydroxyester and the internal catalytic action of the secondary and tertiary amines allow the DCN-PEI polymer to easily dissolve in alcohols through the transesterification process, giving the polymer a great deal of potential for producing recyclable FRPs composite. To understand the performance of the recycled fabrics, they were reused by following the same procedure to prepare the regenerated composite laminates. After using a three-point bending test, the regenerated gradient composite laminates showed a peak bending load of  $235 \pm 32.61$  N with flexural stress of  $42.01 \pm 4.02$  MPa, which is significantly comparable with the freshly prepared samples. Since the gradient composites contained all three fibers (jute, carbon, and glass), the flexural properties of the gradient composites after recycling also reflects the performance of individual fibers. In our previous report, we recycled the individual fibers and found promising performances [21]. Furthermore, after dissolving the polymer from the composites, a slight polymer residue remains on the surface of the recycled fibers (Fig. 6),

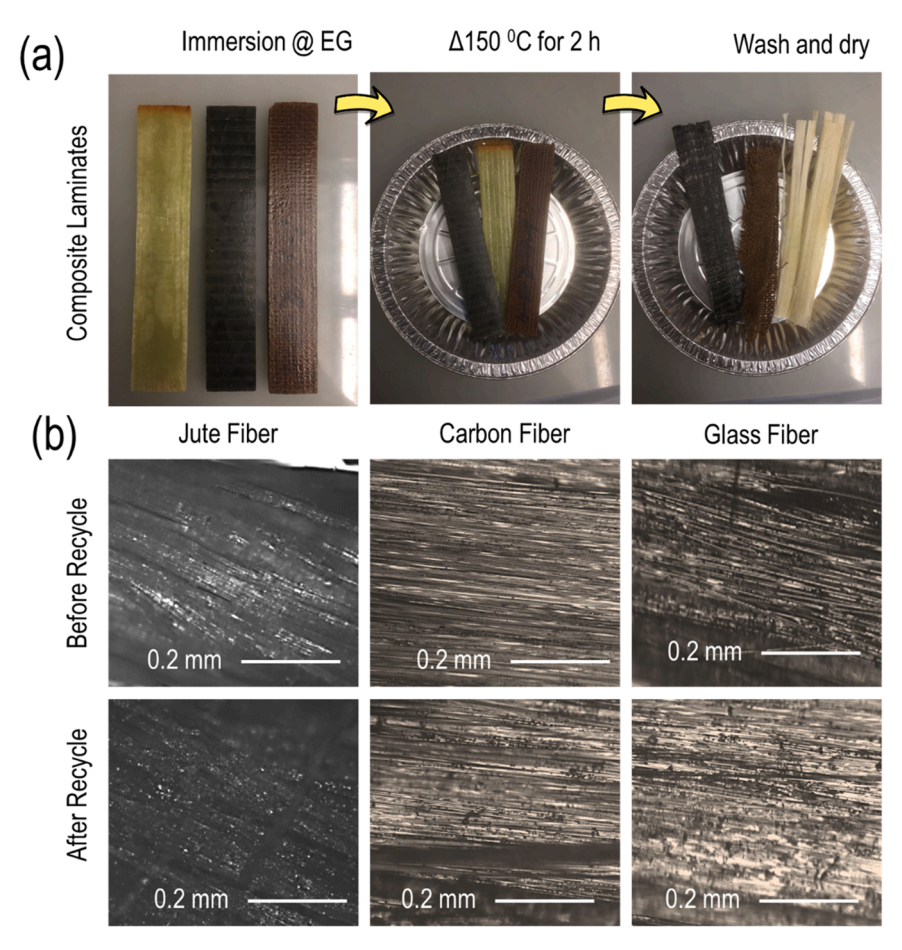


Fig. 6. (a) Photographs exhibiting the chemical recycling process of laminated fabrics, and (b) optical microscopic images of original fabrics (upper column) and chemically recycled fabrics (lower column).

resulting in the stickiness of fibers which could be improved by avoiding manual wash but adopting machine washing. The polymer we used for lamination is a self-healing polymer, so the residue polymer particles can form a bond with the fresh polymers while re-composition through self-healing properties. As a result, the composites prepared by the recycled fibers showed comparable mechanical properties with the freshly prepared samples.

#### 4. Conclusions

Natural fibers have high potential as renewable reinforcement for polymers; however, their lower load-carrying capacity than synthetic fibers significantly limits the wide application in fiber-reinforced polymer composites. In this study, a hybrid reinforcement strategy has been used by combining synthetic fibers and natural fibers in laminated composites in a gradient pattern to overcome the limitations of natural fibers. Particularly, hybrid fibers are arranged in a gradient manner in the order of carbon fiber, glass fiber, and natural fiber from the surface to the mid-plane to match the bending stress distribution in laminated composite under transverse bending load. It is found that the laminated composites with hybrid gradient reinforcement exhibited mechanical properties similar to or slightly higher than those of the laminates reinforced by entirely carbon fibers or glass fibers but much higher, about 550 %, than those with entirely natural fibers reinforcement. Because of the use of shape memory and self-healing thermoset polymer as the matrix, the laminated composites demonstrated self-healing, recycling, and shape memory properties. Furthermore, the fibers recycled through the wet recycling approach by solvent were used to prepare laminated composites again, which exhibited mechanical and functional

properties similar to those of virgin fiber-reinforced laminates. This study shows that the idea of using hybrid fiber reinforcement by arranging them in a gradient manner has a good potential to use natural fibers in load-bearing engineering structures.

## Ethical approval and consent to participate

All authors state that they adhere to the Ethical Responsibilities of Authors. In addition, the work is compliance with ethical standards.

## Consent for publication

All authors listed in this article agree to publish the paper.

## CRediT authorship contribution statement

SM conducted composite preparation and testing and wrote the first draft of the manuscript; JK participated in composite preparation and testing; JD participated in composite preparation and testing; RAS participated in composite preparation; GL conceptualized and supervised the research, obtained funding, and revised the manuscript.

## **Funding**

This work is funded by the US National Science Foundation under Grant Number OIA-1946231 and the Louisiana Board of Regents for the Louisiana Materials Design Alliance (LAMDA), the US National Science Foundation under grant number 1736136, and the US National Science Foundation under grant number 2051050.

#### **Declaration of Competing Interest**

The authors declare that they have no known competing financial interests or personal relationships that could have appeared to influence the work reported in this paper.

#### **Data Availability**

Data will be made available on request.

#### Acknowledgment

The authors would like to thank the Advanced Manufacturing and Machining Facility (AMMF) at Louisiana State University for providing the facilities to cut our samples.

## Appendix A. Supporting information

Supplementary data associated with this article can be found in the online version at doi:10.1016/j.mtcomm.2023.105950.

#### References

- [1] A.A. Horton, Plastic pollution: when do we know enough, J. Hazard. Mater. 422 (2022), 126885, https://doi.org/10.1016/j.jhazmat.2021.126885.
- [2] M.S. Bank, et al., Global plastic pollution observation system to aid policy, Environ. Sci. Technol. 55 (12) (2021) 7770–7775, https://doi.org/10.1021/acs. est.1c00818.
- [3] H.V. Ford, et al., The fundamental links between climate change and marine plastic pollution, Environ. Sci. Technol. 806 (2022), 150392, https://doi.org/10.1016/j. scitoteny.2021.150392.
- [4] R. Stafford, P.J. Jones, Viewpoint–Ocean plastic pollution: a convenient but distracting truth? Mar. Policy 103 (2019) 187–191, https://doi.org/10.1016/j. marpol.2019.02.003.
- [5] J.L. Lavers, A.L. Bond, C. Rolsky, Far from a distraction: plastic pollution and the planetary emergency, Biol. Conserv. 272 (2022), 109655, https://doi.org/ 10.1016/j.biocon.2022.109655.
- [6] J. Hopewell, R. Dvorak, E. Kosior, Plastics recycling: challenges and opportunities, Philos. Trans. R. Soc. Lond. B. Biol. Sci. 364 (1526) (2009) 2115–2126, https://doi. org/10.1098/rstb.2008.0311.
- [7] G. Lu, et al., Bio-based epoxy thermoset containing stilbene structure with ultrahigh T g and excellent flame retardancy, Polym. (Korea) 45 (4) (2021) 581–591, https://doi.org/10.7317/pk.2021.45.4.581.
- [8] M.R. Johansen, T.B. Christensen, T.M. Ramos, K. Syberg, A review of the plastic value chain from a circular economy perspective, J. Environ. Manag. 302 (2022), 113975, https://doi.org/10.1016/j.jenvman.2021.113975.
- [9] S. Mahmud, Y. Long, M. Abu Taher, H. Hu, R. Zhang, J. Zhu, Fully Bio-based microcellulose incorporated poly (butylene 2, 5-furandicarboxylate) transparent composites: preparation and characterization, Fibers Polym. 21 (7) (2020) 1550–1559, https://doi.org/10.1007/s12221-020-9610-8.
- [10] S. Mahmud, Y. Long, J. Wang, J. Dai, R. Zhang, J. Zhu, Waste cellulose fibers reinforced polylactide toughened by direct blending of epoxidized soybean oil, Fibers Polym. 21 (12) (2020) 2949–2961, https://doi.org/10.1007/s12221-020-0111-6.
- [11] M.A. Muflikhun, T. Yokozeki, T. Aoki, The strain performance of thin CFRP-SPCC hybrid laminates for automobile structures, Compos. Struct. 220 (2019) 11–18, https://doi.org/10.1016/j.compstruct.2019.03.094.
- [12] M.A. Muflikhun, B. Fiedler, Failure prediction and surface characterization of GFRP laminates: a study of stepwise loading, Polymers 14 (20) (2022) 4322. . [Online]. Available: (https://www.mdpi.com/2073-4360/14/20/4322).
- [13] O. Faruk, A.K. Bledzki, H.P. Fink, M. Sain, Progress report on natural fiber reinforced composites, Macromol. Mater. Eng. 299 (1) (2014) 9–26, https://doi. org/10.1002/maps.2013.00008
- [14] S. Mahmud, Y. Long, Y. Yang, J. Huang, R. Zhang, J. Zhu, The consequence of epoxidized soybean oil in the toughening of polylactide and micro-fibrillated cellulose blend, Polym. Sci. Ser. A 61 (6) (2019) 832–846, https://doi.org/ 10.1134/S0965545×2001006X.
- [15] C. Dong, I.J. Davies, Flexural strength of bidirectional hybrid epoxy composites reinforced by E glass and T700S carbon fibres, Compos. B. Eng. 72 (2015) 65–71, https://doi.org/10.1016/j.compositesb.2014.11.031.
- [16] L. Ferrante, et al., Behaviour of woven hybrid basalt-carbon/epoxy composites subjected to laser shock wave testing: preliminary results, Compos. B. Eng. 78 (2015) 162–173, https://doi.org/10.1016/j.compositesb.2015.03.084.
- [17] R. Yan, R. Wang, C.-W. Lou, J.-H. Lin, Low-velocity impact and static behaviors of high-resilience thermal-bonding inter/intra-ply hybrid composites, Compos. B. Eng. 69 (2015) 58–68, https://doi.org/10.1016/j.compositesb.2014.09.021.

- [18] F. Sarasini, et al., Damage tolerance of carbon/flax hybrid composites subjected to low velocity impact, Compos. B. Eng. 91 (2016) 144–153, https://doi.org/ 10.1016/j.compositesb.2016.01.050.
- [19] B. Gangil, L. Ranakoti, S. Verma, T. Singh, S. Kumar, Natural and synthetic fibers for hybrid composites, Hybrid. Fiber Compos.: Mater. Manuf. Process Eng. (2020) 1–15, https://doi.org/10.1002/9783527824571.ch1.
- [20] A.D. Nugraha, M.I. Nuryanta, L. Sean, K. Budiman, M. Kusni, M.A. Muflikhun, Recent progress on natural fibers mixed with CFRP and GFRP: properties, characteristics, and failure behaviour, Polymers 14 (23) (2022) 5138 ([Online]. Available), (https://www.mdpi.com/2073-4360/14/23/5138).
- [21] X. Feng, G. Li, Room-temperature self-healable and mechanically robust thermoset polymers for healing delamination and recycling carbon fibers, ACS Appl. Mater. Interfaces 13 (44) (2021) 53099–53110, https://doi.org/10.1021/ acsami.lc16105.
- [22] S. Utekar, V. Suriya, N. More, A. Rao, Comprehensive study of recycling of thermosetting polymer composites-driving force, challenges and methods, Compos. B. Eng. 207 (2021), 108596, https://doi.org/10.1016/j. compositesb.2020.108596.
- [23] M.A. Muflikhun, R. Higuchi, T. Yokozeki, T. Aoki, Delamination behavior and energy release rate evaluation of CFRP/SPCC hybrid laminates under ENF test: corrected with residual thermal stresses, Compos. Struct. 236 (2020), 111890, https://doi.org/10.1016/j.compstruct.2020.111890.
- [24] M.A. Muflikhun, T. Yokozeki, Steel plate cold commercial carbon fiber reinforced plastics hybrid laminates for automotive applications: curing perspective with thermal residual effect, J. Mater. Res. Technol. 14 (2021) 2700–2714, https://doi. org/10.1016/j.jmrt.2021.07.152.
- [25] G. Li, W. Xu, Thermomechanical behavior of thermoset shape memory polymer programmed by cold-compression: testing and constitutive modeling, J. Mech. Phys. Solids 59 (2011) 1231–1250. (https://doi.org/10.1016/j.jmps.2011.03.001).
- [26] G. Li, A. Wang, Cold, warm, and hot programming of shape memory polymers, J. Polym. Sci. Part B: Polym. Phys. 54 (2016) 1319–1339. (https://doi.org/10.1 002/polb.24041).
- [27] J.K. Oleiwi, Q.A. Hamad, H.J.A. Rahman, Study thermal behavior of heat cure poly (methyl methacrylate) reinforced by bamboo and rice husk powders for denture applications, Eng. Sci. 11 (2018) 417–425.
- [28] D. Cho, H.S. Lee, S.O. Han, Effect of fiber surface modification on the interfacial and mechanical properties of kenaf fiber-reinforced thermoplastic and thermosetting polymer composites, Compos. Interfaces 16 (7–9) (2009) 711–729, https://doi.org/10.1163/092764409x12477427307537.
- [29] N. Nurazzi, et al., Thermogravimetric analysis properties of cellulosic natural fiber polymer composites: a review on influence of chemical treatments, Polymers 13 (16) (2021) 2710, https://doi.org/10.3390/polym13162710.
- [30] Q. Shi, C. Zhou, Y. Yue, W. Guo, Y. Wu, Q. Wu, Mechanical properties and in vitro degradation of electrospun bio-nanocomposite mats from PLA and cellulose nanocrystals, Carbohydr. Polym. 90 (1) (2012) 301–308, https://doi.org/10.1016/ i.carbool.2012.05.042.
- [31] X. Feng, G. Li, Catalyst-free β-hydroxy phosphate ester exchange for robust fireproof vitrimers, Chem. Eng. J. 417 (2021), 129132, https://doi.org/10.1016/j. cei/2021.129132
- [32] S.K. Paswan, et al., Optimization of structure-property relationships in nickel ferrite nanoparticles annealed at different temperature, J. Phys. Chem. Solids 151 (2021), 109928, https://doi.org/10.1016/j.jpcs.2020.109928.
- [33] S. Yousef, J. Eimontas, N. Striūgas, M.A. Abdelnaby, Influence of carbon black filler on pyrolysis kinetic behaviour and TG-FTIR-GC-MS analysis of glass fibre reinforced polymer composites, Energy 233 (2021), 121167, https://doi.org/ 10.1016/j.energy.2021.121167.
- [34] C. Chen, X. Bu, D. Huang, Y. Huang, H. Huang, Thermal decomposition and kinetics analysis of microwave pyrolysis of Dunaliella salina using composite additives, Bioenergy Res. 13 (4) (2020) 1205–1220, https://doi.org/10.1007/ s12155.020.10150.7
- [35] M.K.M. Haafiz, A. Hassan, Z. Zakaria, I.M. Inuwa, M.S. Islam, M. Jawaid, Properties of polylactic acid composites reinforced with oil palm biomass microcrystalline cellulose, Carbohydr. Polym. 98 (1) (2013) 139–145, https://doi. org/10.1016/j.carbpol.2013.05.069.
- [36] P. Qu, Y. Gao, G. Wu, L. Zhang, Nanocomposites of poly (lactic acid) reinforced with cellulose nanofibrils, BioResources 5 (3) (2010) 1811–1823.
- [37] S.-C. Lee, S.-T. Jeong, J.-N. Park, S.J. Kim, G.-J. Cho, A study on mechanical properties of carbon fiber reinforced plastics by three-point bending testing and transverse static response, J. Mater. Process. Technol. 201 (1) (2008) 761–764, https://doi.org/10.1016/j.jmatprotec.2007.11.248.
- [38] G. Ji, Z. Ouyang, G. Li, Effects of bondline thickness on mode-II interfacial laws of bonded laminated composite plate, Int. J. Fract. 168 (2011) 197–207, https://doi. org/10.1007/s10704-010-9571-9.
- [39] Y. Yuan, et al., Multiply fully recyclable carbon fibre reinforced heat-resistant covalent thermosetting advanced composites, Nat. Commun. 8 (1) (2017) 14657, https://doi.org/10.1038/ncomms14657.
- [40] Y. Wang, et al., Chemical recycling of carbon fiber reinforced epoxy resin composites via selective cleavage of the carbon–nitrogen bond, ACS Sustain. Chem. Eng. 3 (12) (2015) 3332–3337, https://doi.org/10.1021/acssuschemeng.5b00949.
- [41] A. Yamaguchi, et al., Recyclable carbon fiber-reinforced plastics (CFRP) containing degradable acetal linkages: Synthesis, properties, and chemical recycling, J. Polym. Sci. Part A: Polym. Chem. 53 (8) (2015) 1052–1059, https://doi.org/10.1002/ pola.27575.